Analysis of ^{1}H–^{14}N polarization transfer experiments in molecular crystals

2005 J. Phys.: Condens. Matter 17 519

(http://iopscience.iop.org/0953-8984/17/3/011)

INSTITUTE OF PHYSICS PUBLISHING JOURNAL OF PHYSICS: CONDENSED MATTER

J. Phys.: Condens. Matter **17** (2005) 519–533 doi:10.1088/0953-8984/17/3/011

Analysis of ^{1}H–^{14}N polarization transfer experiments in molecular crystals

D Kruk[1,2,4], J Altmann[1,3], F Fujara[1], A Gädke[1], M Nolte[1] and A F Privalov[1]

[1] Institut für Festkörperphysik, TU Darmstadt, Hochschulstraße 6, 64289 Darmstadt, Germany
[2] Institute of Physics, Jagiellonian University, Reymonta 4, 30-059 Krakow, Poland
[3] Experimentelle Physik III, Universität Dortmund, 44221 Dortmund, Germany

E-mail: Danuta.Kruk@physik.tu-darmstadt.de

Received 28 September 2004, in final form 8 December 2004
Published 7 January 2005
Online at stacks.iop.org/JPhysCM/17/519

Abstract

A general theoretical description of polarization transfer processes in multi-spin systems containing dipole as well as quadrupole spins is formulated on the background of the Liouville–von Neumann equation. The density operator formalism is used to describe the evolution of an arbitrary spin system due to quadrupole, Zeeman and dipole–dipole interactions. This approach is applied to interpret previously published ^{1}H–^{14}N cross-relaxation NMR experiments for measuring the ^{14}N quadrupole coupling constants of paranitrotoluene (PNT) and trinitrotoluene (TNT) (Nolte *et al* 2002 *J. Phys. D: Appl. Phys.* **35** 939) and new experiments on urea and urotropine. It is demonstrated that according to the complexity of the analysed spin system an appropriate number of spins has to be taken into consideration for a correct description of the cross-relaxation spectra. The work is a part of an extended project aiming for a method which should permit detection of TNT explosive in anti-personnel landmines.

1. Introduction

Zero-field NQR detection of ^{14}N in metal free anti-personal landmines has made some progress as long as its quadrupole frequencies are sufficiently large (3–5 MHz). This is the case when nitrogen is contained within the aromatic ring. For instance, it has been reported that some 50 g of the explosive hexogen (RDX) have been successfully detected by zero-field NQR just using a surface rf coil [2]. However, despite strong efforts [3], one of the explosives intensively used in landmines, trinitrotoluene (TNT), has not been detected by zero-field NQR due to its small quadrupole frequencies of less than 900 kHz.

[4] Author to whom any correspondence should be addressed.

The present work largely refers to a previous paper [1], which presented ^{1}H–^{14}N cross-relaxation (CR) NMR spectra obtained by electronical field cycling spectroscopy on paranitrotoluene (PNT) and trinitrotoluene (TNT). It had been demonstrated that this method is very sensitive for detecting e.g. the TNT NQR spectrum. Thereby, this detection scheme may provide a useful perspective for developing a modified NQR probe for TNT-containing metal-free anti-personnel landmines.

A qualitative interpretation, already given in [1], attributed observed dips in a ^{1}H CR spectrum to matching of Zeeman energy splitting for protons with some energy splitting for nitrogen spins. The polarization transfer from a ^{1}H spin to a neighbouring ^{14}N spin is caused by the mutual dipole–dipole coupling [4, 5]. The present paper is meant to propose a quantitative analysis of the observed CR spectra on a background of the Liouville–von Neumann equation. The time development of the spin density operator for a multi-spin system under the influence of Zeeman, electrical quadrupole and magnetic dipole interactions is considered. The approach is used to make a detailed re-interpretation of the data for PNT and TNT and also of new experimental results on some more nitrogen-containing molecular crystals, namely urea and urotropine. We provide in this work a tool for analysis and interpretation of CR experiments for an arbitrary spin system, linking the efficiency of polarization transfer effects to molecular geometry.

This theory oriented paper is organized such that after a short account of the experimental procedure (section 2), the density operator formalism is reviewed in some detail in the section 3. The application of this treatment to our previous experimental CR results on PNT and TNT as well as to our new data on urea and urotropine is presented in section 4. Section 5 is devoted to a discussion of problems relevant for magnetization transfer processes, like effects of non-equivalent spins involved in polarization transfers within one molecule, a possible polarization transfer to neighbouring molecules and relaxation dynamics of the quadrupole as well as dipolar spins.

For simplicity we use from now on the symbol H instead of ^{1}H and the symbol N instead of ^{14}N to denote the proton and nitrogen spins, respectively.

2. H–N cross-relaxation experiments

Details of the cross-relaxation experiments have been given in [1], so we present only a very short summary here. The experiments were performed using a fast-field-cycling spectrometer. A magnetic field (of about 0.7 T) was applied in a preparation period to polarize the proton spins. Next, the magnetic field is reduced to a low cross-relaxation field, B_{CR}, which is varied for searching for H–N polarization transfer effects. After switching to a detection field (of about 1 T), the remaining proton magnetization is recorded. The timing diagram of the experiment is presented in figure 1 of [1].

3. Theory of polarization transfer effects for H–N spin systems

This section is devoted to a straightforward theoretical description of polarization transfer effects appropriate to a subsequent treatment for the series of spin systems H–N, H–N–H, N–H–N and N–H–N–H–N, linking the efficiency of the cross-relaxation processes to the structure of the investigated molecules. We discuss single- as well as double-quantum mechanisms of the proton polarization transfer for systems containing several proton and nitrogen spins. The description presented here can be treated as an extension of the approach of [4] to an arbitrary molecular system containing spins $I = 1/2$ as well as quadrupole spins S.

The dynamics of an ensemble of nuclear spins under a Hamiltonian H is governed by the Liouville–von Neumann equation [4–8]:

$$\frac{\mathrm{d}}{\mathrm{d}t}\rho(t) = -\mathrm{i}[H, \rho(t)] \tag{1}$$

where $\rho(t)$ is the density operator for the considered quantum system. The Hamiltonian H appropriate for the system containing N_I proton spins, $I = \frac{1}{2}$, coupled to N_S nitrogen spins, $S = 1$, consists of Zeeman interactions with the static magnetic field (H_{Z}^I and H_{Z}^S for the spins I and S, respectively) and internal spin interactions, i.e. quadrupole (H_{Q}^S) interactions for the spin S and dipole–dipole couplings (H_{DD}^{II}, H_{DD}^{IS}, H_{DD}^{SS}) between pairs of the spins:

$$H = \sum_{i=1}^{N_I} H_{\mathrm{Z}}^I(I_i) + \sum_{j=1}^{N_S} H_{\mathrm{Z}}^S(S_j) + \sum_{j=1}^{N_S} H_{\mathrm{Q}}^S(S_j) + \sum_{i_1,i_2=1,i_2<i_1}^{N_I} H_{\mathrm{DD}}^{II}(I_{i_1}, I_{i_2}) + \sum_{i=1}^{N_I}\sum_{j=1}^{N_S} H_{\mathrm{DD}}^{IS}(I_i, S_j) + \sum_{j_1,j_2=1,j_2<j_1}^{N_S} H_{\mathrm{DD}}^{SS}(S_{j_1}, S_{j_2}). \tag{2}$$

In the general case of several interactions, all the contributions to the total Hamiltonian have to be considered in the same reference frame. For the purpose of describing the results of our experiments performed in the laboratory frame (L), determined by the direction of the external magnetic field, we choose the (L) coordinate system as the reference frame. The Zeeman couplings for the spins I and S take in the laboratory frame the simple form

$$H_{\mathrm{Z}}^{P(L)} = \gamma_P B_0 P_z \qquad P = I, S \tag{3}$$

where γ_P is the appropriate gyromagnetic factor.

The quadrupole coupling, H_{Q}^S, may be expressed in the (L) frame by a sum over products of the components of two irreducible spherical tensors, in the following way [6–8]:

$$H_{\mathrm{Q}}^{S(L)} = \tfrac{1}{2}\sqrt{\tfrac{3}{2}}a_{\mathrm{Q}}^S \sum_{m=-2}^{2} (-1)^m A_m^{S(L)} T_{2,-m}(S) \tag{4}$$

where $T_{2,-m}(S)$ are components of the rank two spin tensor operator, $T_{2,0}(S) = \frac{1}{\sqrt{6}}[3S_z^2 - S(S+1)]$, $T_{2,\pm1}(S) = \mp\frac{1}{2}[S_z S_\pm + S_\pm S_z]$, $T_{2,\pm2}(S) = \frac{1}{2}S_\pm S_\pm$. The quadrupole coupling constant a_{Q}^S for the spin S is defined as $a_{\mathrm{Q}}^S = e^2 q_S Q_S / h$, where the symbols have their usual meaning. The exact form of the space tensor elements A_m^S depends upon the chosen reference frame it is expressed in. For clarity of further considerations we define at this point a molecular frame, denoted by (M). The molecular frame is a reference frame fixed on the molecule and may be chosen arbitrarily. We chose as the molecular frame the principal axis system (PAS) of the electric field gradient, (P) frame, for one of the spins S and denote this distinguished spin as S_1. Thus one can write $(P_1) = (M)$. Transformations of the tensor components $A_m^{S_i}$, [9], from the PAS of the electric field gradient, (P_i), for the spin S_i to the laboratory frame occur through two sets of Wigner rotation matrices:

$$A_m^{S_i(L)} = \sum_{n=-2}^{2}\sum_{k=-2}^{2} A_k^{(P_i)} D_{k,n}^2(\Omega_{P_i M}) D_{n,m}^2(\Omega_{\mathrm{ML}}). \tag{5}$$

In the first step the tensor functions $A_k^{(P_i)}$ are transformed from the (P_i) frame to the (M) frame through the set of Euler angles $\Omega_{P_i M} \equiv \{\alpha_{P_i M}, \beta_{P_i M}, \gamma_{P_i M}\}$; in particular, for the spin S_1 one has $\Omega_{P_1 M} \equiv 0$. The second transformation is performed between the molecular and laboratory frames and expressed in terms of the Euler angles $\Omega_{\mathrm{ML}} \equiv \{\alpha_{\mathrm{ML}}, \beta_{\mathrm{ML}}, \gamma_{\mathrm{ML}}\}$ common for all spins S_i and denoted from now as $\Omega_{\mathrm{ML}} \equiv \Omega$. For equivalent spins all the functions $A_k^{(P_i)}$ are

the same, $A_k^{(P_i)} = A_k^{(P)}$, and have the form $A_0^{(P)} = 1$, $A_{\pm1}^{(P)} = 0$, $A_{\pm2}^{(P)} = \frac{1}{\sqrt{6}}\eta$ where η is the asymmetry parameter. The orientations of the P_i frames for the particular quadrupole couplings of the S_i spins with respect to the distinguishable molecular frame, P_1, are determined by the molecular geometry and are independent of the molecular orientation encoded in the angle Ω.

The dipole–dipole interactions being expressed by second rank tensors as well can be treated in a similar manner. The I–S dipole–dipole Hamiltonian takes in the laboratory frame the form [6–8]

$$H_{\mathrm{DD}}^{(L)}(I,S) = a_{\mathrm{D}}^{IS} \sum_{m=-2}^{2} (-1)^m F_m^{IS(L)} T_{2,-m}(I,S). \tag{6}$$

The components $T_{2,-m}(I,S)$ of the two-spin tensor operator have the form $T_{2,0} = \frac{1}{\sqrt{6}}[2I_zS_z - \frac{1}{2}(I_+S_- + I_-S_+)]$, $T_{2,\pm1} = \mp\frac{1}{2}[I_zS_\pm + I_\pm S_z]$, $T_{2,\pm2} = \frac{1}{2}I_\pm S_\pm$, and the dipolar coupling constant is defined as $a_{\mathrm{D}}^{IS} = \sqrt{6}\frac{\mu_0}{4\pi}\frac{\gamma_I\gamma_S\hbar^2}{r_{IS}^3}$ where r_{IS} is the inter-spin distance; the other symbols have their usual meaning. The relationship of the tensor components $F_m^{IS(L)}$ and $F_k^{(\mathrm{DD}_{IS})}$, defined respectively in the laboratory frame and the frame determined by the dipole–dipole I–S axis, (DD_{IS}), can be obtained in a full analogy to the transformation of equation (5) via the molecular co-ordinate system (M):

$$F_m^{IS(L)} = \sum_{n=-2}^{2}\sum_{k=-2}^{2} F_k^{(\mathrm{DD}_{IS})} D_{k,n}^2(\Omega_{\mathrm{DD}_{IS}M}) D_{n,m}^2(\Omega). \tag{7}$$

The set of Euler angles $\Omega_{\mathrm{DD}_{IS}M} \equiv \{\alpha_{\mathrm{DD}_{IS}M}, \beta_{\mathrm{DD}_{IS}M}, \gamma_{\mathrm{DD}_{IS}M}\}$ describes the orientation of the dipole–dipole co-ordinate system for the pair of interacting spins I–S with respect to the molecular frame. Since for an arbitrary pair of spins one has $F_0^{(\mathrm{DD})} = 1$, $F_{\pm1,\pm2}^{(\mathrm{DD})} = 0$ equation (7) can be simplified to the form

$$F_m^{IS(L)} = \sum_{n=-2}^{2} D_{0,n}^2(0,\theta_{IS},\varphi_{IS}) D_{n,m}^2(\Omega) \tag{7a}$$

where the link between the Euler and the polar angles is employed: $\beta_{\mathrm{DD}_{IS}M} = \theta_{IS}$, $\gamma_{\mathrm{DD}_{IS}M} = \varphi_{IS}$. The angles θ_{IS} and φ_{IS} associated with the I–S dipole–dipole coupling are also (in analogy to Ω_{P_iM}) determined by the molecular geometry and remain unchanged for an arbitrary molecular orientation. All the above considerations performed for a pair of spins I_i–S_j (H–N) are fully applicable for the I_i–I_j (H–H) and S_i–S_j (N–N) dipole–dipole interactions.

The dipole–dipole interactions providing a coupling between the proton and nitrogen spins are responsible for the H–N cross-relaxation effects. The efficiency of the proton polarization transfer depends on the strength of the particular dipolar couplings, determined by the inter-spin distances, $r_{I_iS_j}$, and the molecular geometry entering the dipole–dipole Hamiltonians through the Euler angles $\theta_{I_iS_j}, \varphi_{I_iS_j}$.

We now turn to the Liouville description of spin dynamics. The expectation value of an observable Q over the ensemble of spin systems described by a time-independent Hamiltonian H can be obtained from the relation

$$\langle Q(t)\rangle = \mathrm{Tr}\{\rho(t)Q\} = \sum_{r,s=1}^{N} a_{rs}\exp\{-\mathrm{i}\omega_{rs}t\} \tag{8}$$

with the amplitude a_{rs} given by

$$a_{rs} = \langle r|\rho(0)|s\rangle\langle s|Q|r\rangle. \tag{9}$$

The coefficients a_{rs} are products of the elements of the observable, $Q_{sr} = \langle s|Q|r\rangle$, and the elements of the initial density operator, $\rho(0)_{rs} = \langle r|\rho(0)|s\rangle$, both expressed in the eigenbasis of the Hamiltonian H.

The strong magnetic field applied in the preparation period of the cross-relaxation experiments determines the initial density operator, $\rho(0)$, for the considered system. In the limit of high temperature approximation, which is easy fulfilled at room temperature, the initial equilibrium density operator is proportional to a combination of the I_z and S_z operators:

$$\rho(0) = \frac{1}{Z}\exp\left(-\left(\sum_{i=1}^{N_{Ii}} H_{\mathrm{Z}}^{I_i} + \sum_{j=1}^{N_S} H_{\mathrm{Z}}^{S_j}\right)/k_{\mathrm{B}}T\right) \propto \sum_{i=1}^{N_I} I_{iz} + \frac{\gamma_S}{\gamma_I}\sum_{j=1}^{N_S} S_{jz}.$$

The ensemble partition function is $Z = (2I+1)^{N_I}(2S+1)^{N_S}$, while k_{B} is the Boltzmann constant.

To obtain the eigenstates and the corresponding eigenvalues (energy levels) for the considered system, one has to diagonalize the Hamiltonian of equation (2) with all the terms expressed in the laboratory frame. We use for the diagonalization a matrix representation of the Hamiltonian in the Zeeman basis set $|n\rangle = |m_{S_1}, \ldots, m_{S_{N_S}}, m_{I_1}, \ldots, m_{I_{N_I}}\rangle$, where m_{S_j} and m_{I_i} are the magnetic quantum numbers for the nitrogen spin S_j and the proton spin I_i, respectively. The role of the dipole–dipole interaction as the mechanism causing the polarization transfer manifests itself clearly through the form of its matrix representation: the dipole–dipole Hamiltonian provides a coupling between two sub-sets of the basis functions corresponding to different values of the m_I quantum number: $\Delta m_I = \pm 1$.

In the experiment the proton magnetization is detected, thus the observable Q refers to a superposition of the operators I_{iz}. Using the representation of the eigenfunctions $|\psi_r\rangle$ of the Hamiltonian H for a given molecular orientation Ω in terms of the Zeeman basis functions $|n\rangle$:$|\psi_r\rangle = \sum_{n=1}^{N} c_{rn}(\Omega)|n\rangle$ (N denotes the number of eigenstates), one can write the expression for the set of coefficients $a_{rs}(\Omega)$ (equation (9)) in the form

$$a_{rs}(\Omega) \cong \sum_{n,m=1}^{N}\left\{\langle n|I_{1z} + \cdots + I_{N_Iz}|m\rangle + \frac{\gamma_S}{\gamma_I}\langle n|S_{1z} + \cdots + S_{N_Sz}|m\rangle\right\}(c_{rn}^* c_{sm})(\Omega)$$
$$\times \sum_{n,m=1}^{N}\langle m|I_{1z} + \cdots + I_{N_Iz}|n\rangle(c_{sm}^* c_{rn})(\Omega). \tag{10}$$

Thus the proton magnetization of molecules oriented with respect to the laboratory frame under the angle Ω is given by

$$\langle I_z(t)\rangle(\Omega) \cong \sum_{r,s=1}^{N}\left(\sum_{n=1}^{N}\langle n|I_{1z} + \cdots + I_{N_Iz}|n\rangle(c_{rn}^* c_{sn})(\Omega)\right)^2 \exp(-\mathrm{i}\omega_{rs}t)$$
$$+ \frac{\gamma_S}{\gamma_I}\sum_{r,s=1}^{N}\left\{\left(\sum_{n=1}^{N}\langle n|I_{1z} + \cdots + I_{N_Iz}|n\rangle(c_{rn}^* c_{sn})(\Omega)\right)\right.$$
$$\left.\times\left(\sum_{n=1}^{N}\langle n|S_{1z} + \cdots + S_{N_Sz}|n\rangle(c_{rn}^* c_{sn})(\Omega)\right)\right\}\exp(-\mathrm{i}\omega_{rs}t) \tag{11}$$

where we have taken into account that the operators I_z and S_z are diagonal in the Zeeman representation, such that one can set $n = m$. Since the Zeeman states with $m_S = 1$ and -1 contribute in an equivalent manner to the eigenstates of the I–S system, the second term in equation (11) vanishes. The transition frequencies, $\omega_{rs} = E_r - E_s$, are determined by the eigenvalues E_r, E_s of the eigenstates $|r\rangle$, $|s\rangle$, respectively.

The detected proton magnetization results as a sum of responses from molecules with different orientations in the sample, thus in the last step one needs to perform an averaging over all molecular orientations. The idea to introduce the molecular frame (M) as an intermediate step for the transformations of the quadrupole and dipole–dipole interactions from their PAS systems to the laboratory frame allows one to focus on only one set of Euler angles Ω in the averaging procedure. The resulting proton magnetization $\langle I_z(t)\rangle = \overline{\langle I_z(t)\rangle(\Omega)}$ (the bar denotes the averaging over molecular orientations) is affected by the molecular geometry through the amplitudes a_{rs} determined by the interactions (quadrupole and dipole–dipole) as they depend on internal molecular distances and angles.

Proton polarization is taken over by the nitrogen spins under certain conditions. Whenever the transition energy of the proton spin I (essentially determined by its Zeeman interaction) is equal to the transition energy of the nitrogen spin S (determined by the Zeeman and quadrupole couplings), the dipole–dipole interaction, $H_{\mathrm{DD}}(I, S)$, can cause polarization transfer processes. The proton polarization is transferred through single-quantum transitions, $|\Delta m_I| = 1$, associated with appropriate transitions of the nitrogen spin, $\Delta m_S = -\Delta m_I$. If more proton spins, I_1, I_2, coupled to the nitrogen spin S, contribute to the polarization transfer, the proton magnetization can be taken over not only through single-quantum transitions but also through the double-quantum channel: $\Delta m_{I_1} + \Delta m_{I_2} = -\Delta m_S = \pm 2$. The presence of more nitrogen spins increases the effectiveness of the magnetization transfer because more polarization transfer pathways are available for the protons.

In the next section we apply this theoretical approach to interpretation of H–N cross-relaxation experiments on a series of molecules: PNT, TNT, urea and urotropine[5].

4. Analysis of experimental results

Two of the systems discussed below, PNT and TNT, have already been the subject of a previous publication where the emphasis had been put on the experiment. Here, we start our analysis from PNT and urea. We consider polarization transfer effects in these molecules on the background of a three-spin (H–N–H) approach, sufficient to explain the modulation of the proton magnetization due to single- and double-quantum transitions. In the case of TNT, a five-spin system (N–H–N–H–N) turns out to be necessary to explain the spectra. Finally, urotropine stands for a case where an even larger number of coupled spins should be incorporated into the description of the cross-relaxation processes, but we also consider the magnetization transfers within a three-spin system (H–N–H), and discuss this simplification.

The molecules are treated as being isolated, i.e. we do not consider polarization transfers to atoms of neighbouring molecules. In the analysis we focus attention on the most important aspects of the polarization transfer processes: the single- and double-quantum mechanisms and the effects of including more proton as well as nitrogen spins participating in the magnetization transfer. We treat the experimental data as a material for calculations illustrating our approach.

4.1. Paranitrotoluene (PNT)

The proton magnetization for PNT has been measured versus the cross-relaxation magnetic field B_{CR} for two durations of the cross-relaxation period $t_{\mathrm{CR}} = 15$ and 60 s, as presented in [1]. The observed magnetization dips are created by single- as well as double-quantum transitions.

One can distinguish in the PNT molecule three non-equivalent proton groups. The first group, mainly involved in the proton–nitrogen polarization transfer, contains two proton spins

[5] Experimental data of two of these systems, urea and urotropine, are presented for the first time.

closest to the nitrogen. The second group also contains two protons, but more distant from the nitrogen, while the third one corresponds to the methyl group protons.

To explain the polarization transfer we consider the H–N–H spin system, marked in figure 1(c), consisting of the nitrogen spin S and the two closest proton spins I_1 and I_2. According to section 3, the description of polarization transfer effects in a system containing two proton spins and one nitrogen spin requires a Zeeman basis set consisting of 12 functions formed as $|n\rangle = |m_S, m_{I_1}, m_{I_2}\rangle$, where m_S, m_{I_1} and m_{I_2} are the magnetic quantum numbers of the particular spins. The Hamiltonian H contains the Zeeman couplings $H_Z^{I_1}$, $H_Z^{I_2}$, H_Z^S, the quadrupole interaction H_Q^S and the dipole–dipole couplings $H_{DD}^{I_1S}$, $H_{DD}^{I_2S}$, $H_{DD}^{I_1I_2}$, where the last one is of minor importance for PNT molecules due to the relatively long distance between the interacting proton spins. Energy level crossings, corresponding to the positions of proton magnetization dips, appear for certain values of the magnetic field determined by the parameters of the nitrogen quadrupole coupling. We have obtained from our model that the positions of the detected magnetization dips correspond to the quadrupole coupling constant $a_Q = e^2qQ/h = 1.35$ MHz and the asymmetry parameter $\eta = 0.38$. To visualize the polarization transfer processes on the background of the transitions of the participating spins, we present in figure 1(a) the energy level structure for the spin subsystem H–N. The energy levels depend on the orientation of the molecular frame (the principal axis system of the electric field gradient) relative to the laboratory frame. Figure 1(a) shows the energy levels for the molecular orientation parallel to the external magnetic field ($\Omega = 0$); the distribution of molecular orientations causes a spread of the energy level crossings, reflected by widths of the magnetization dips. The detected single-quantum dips occur due to the three transitions with the energies indicated in figure 1(a). The presence of the second proton spin introduces the double-quantum pathway for the proton magnetization transfer and explains the experimental double-quantum dips. The appropriate energy level structure for the H–N–H spin system ($\Omega = 0$) is shown in figure 1(b), where the energies of single- and double-quantum processes are indicated; three transitions also contribute to the double-quantum polarization transfer. The energies of the transitions responsible for the single- as well as the double-quantum polarization transfer agree with the positions of the experimental single- and double-quantum magnetization dips. In figure 1(c) we present the experimental and theoretically predicted proton magnetization as a function of the magnetic field. The efficiency of the polarization transfer effects is linked to the molecular geometry. The calculations presented here have been performed using the crystallographic data from [10]. The two proton–nitrogen distances are equal, 2.65 and 2.57 Å; we have used the average value of 2.6 Å. The angle between the two N–H dipole–dipole axes is 122°. The z component of the nitrogen electric field gradient (EFG) lies almost exactly along the C–N bond, while the y axis has been determined to lie essentially normal to the plane of the NO_2 group [11].

The polarization of the remaining proton spins is transferred to the nitrogen spin much less effectively, because of the significantly larger H–N distances. In general, increasing the number of proton spins contributing to the proton polarization relative to the number of nitrogen spins leads to a decrease of the dip depths. The effects of the ratio between the proton and nitrogen spins are clearly visible for the TNT molecule considered in section 4.3. We come back to this issue in section 5, discussing it in connection with relaxation processes of the participating spins.

4.2. Urea

The urea molecule contains two equivalent NH_2 groups. We analyse the polarization transfer processes within one of them. We consider the H–N–H systems of two protons coupled to

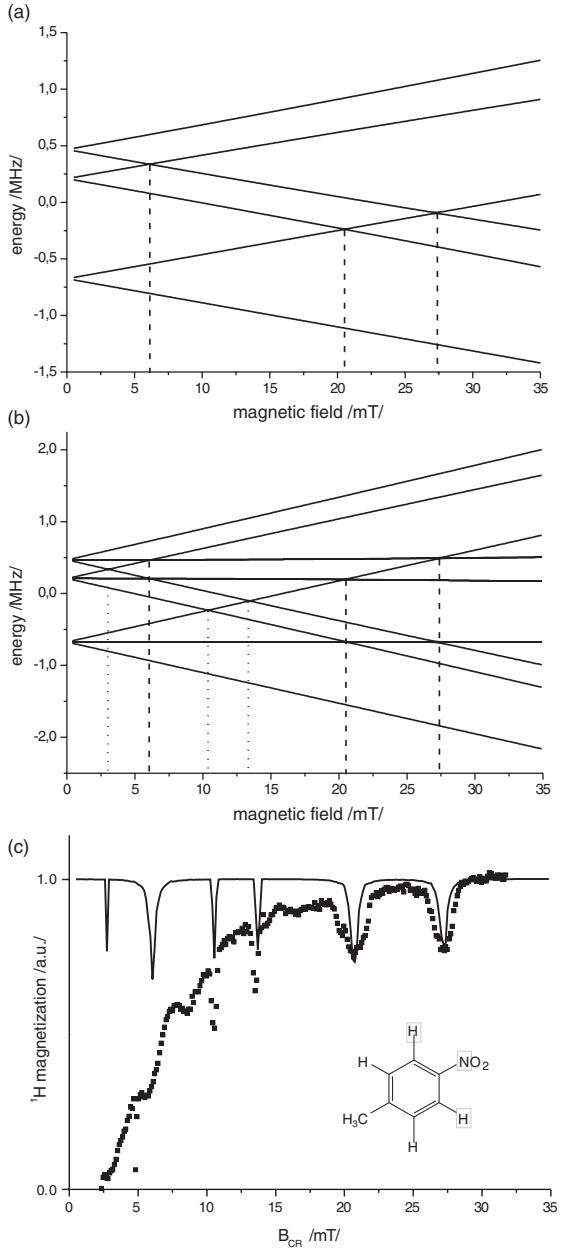

Figure 1. (a) Energy level structure for the H–N subsystem of PNT molecules for the quadrupole coupling constant $a_Q = 1.35$ MHz and the asymmetry parameter $\eta = 0.38$; the relative orientation of the principal axis system of the quadrupole coupling with respect to the laboratory frame is given by $\Omega = 0$. The positions of the energy level crossings correspond to the observed single-quantum transitions for PNT (see (c)). (b) Energy level structure for the H–N–H spin system of PNT: $a_Q = 1.35$ MHz, $\eta = 0.38$; $\Omega = 0$. Energy level crossings corresponding to single- and double-quantum proton transitions are indicated by dashed lines (single quantum) and dotted lines (double quantum). (c) Experimental and calculated proton magnetization as a function of the cross-relaxation magnetic field B_{CR} for PNT, $t_{CR} = 15$ s. The theoretical prediction for the H–N–H spin system (marked in the molecule diagram) is shown as a solid curve: $a_Q = 1.35$ MHz, $\eta = 0.38$.

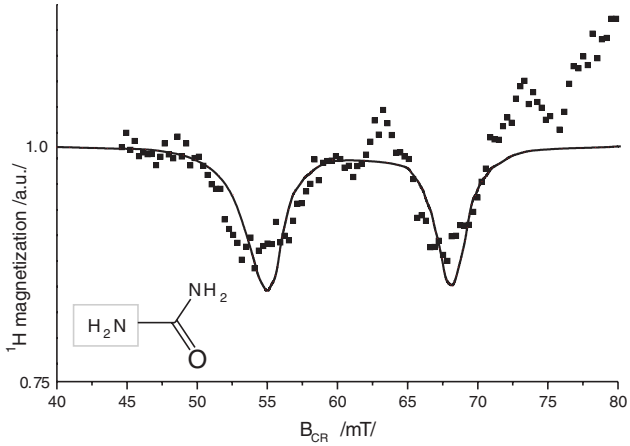

Figure 2. Experimental and calculated proton magnetization as a function of the cross-relaxation magnetic field B_{CR} for urea (the H–N–H spin group is marked in the molecule diagram); squares—experimental data for the cross-relaxation time $t_{CR} = 0.02$ s. The theoretical prediction is shown as a solid curve: $a_Q = 3.46$ MHz, $\eta = 0.29$. The magnetic field range chosen for the cross-relaxation experiment corresponds to single-quantum dips of the proton magnetization.

(This figure is in colour only in the electronic version)

single nitrogen. The experimental data for urea were collected in the range of the magnetic field 45–80 mT, setting the cross-relaxation time t_{CR} to 0.02 s, while the polarization time (the preparation period) was set to 100 s. We have analysed the results in full analogy to the PNT case, calculating the energy level structure and the magnetization development for the H–N–H spin system, marked in figure 2. We have used in the calculations the proton–nitrogen distance of 1 Å, and the HNH angle of 118.6° [12]. The calculations are performed for the electric field gradient with the z axis along the symmetry axis of the NH_2 group. The quadrupole coupling parameters, $a_Q = e^2qQ/h = 3.46$ MHz and $\eta = 0.29$, reflect the positions of the observed proton magnetization dips of the two single-quantum proton transitions. The parameters are in a good agreement with [13] ($a_Q = 3.42$ MHz, $\eta = 0.32$). The comparison between the theoretical curve and the experiments is shown in figure 2.

4.3. Trinitrotoluene (TNT)

The results of the cross-relaxation experiment for TNT have also been presented in [1]. The experiment has been performed for military-grade TNT from a granulated Yugoslav mine sample. The most significant difference between the PNT and TNT data, pointed out in the previous work [1] is the depth of the cross-relaxation dips being much more pronounced in TNT as compared to PNT.

The result is caused by the presence of more nitrogen spins leading to a more efficient proton magnetization transfer. In the first step we have analysed the H–N–H spin subsystem, indicated in figure 3. The quadrupole coupling parameters $a_Q = e^2qQ/h = 1.04$ MHz and $\eta = 0.21$ correspond to the positions of the experimental single- as well as double-quantum dips. The theoretically predicted proton magnetization is presented together with the experimental data in figure 3. In the next step we extend our analysis to the N–H–N–H–N spin system, marked in the molecule diagram in figure 5. To illustrate the role of the additional nitrogen spins we show in figure 4 the energy level structure for the N–H–N spin

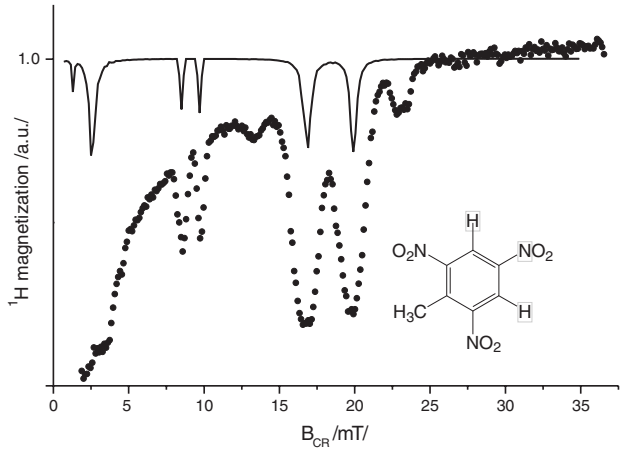

Figure 3. Calculated proton magnetization for the H–N–H subsystem of the TNT molecule (marked in the molecule diagram): $a_Q = 1.04$ MHz, $\eta = 0.21$—solid curve, and experimental results obtained for the cross-relaxation time $t_{CR} = 8$ s—squares.

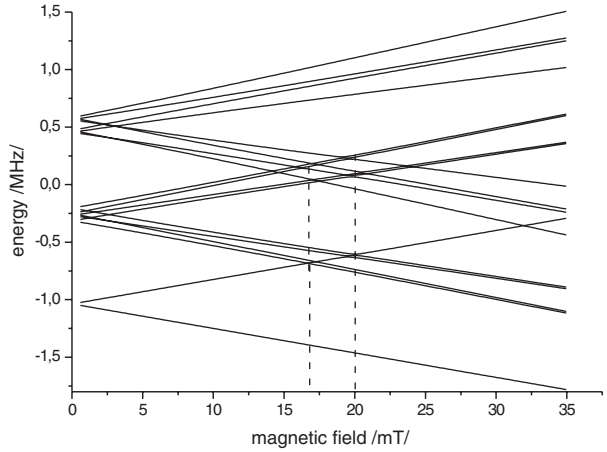

Figure 4. Energy level structure for the N–H–N subsystem of TNT molecules: $a_Q = 1.04$ MHz, $\eta = 0.21$; $\Omega = 0$. Frequencies corresponding to single-quantum proton transitions are indicated.

subsystem, where two nitrogen spins participate in the transfer of the single-proton polarization. The energy level structure explains the effects of more pronounced magnetization dips in comparison to a system containing only one nitrogen spin. The fact that there are more nitrogen spins contributing to taking over the proton magnetization manifests itself through the number of energy level crossings (indicated in figure 4) providing the magnetization transfer channels. Figure 5 shows the experimental data and the calculated proton magnetization (corresponding to the quadrupole parameters $a_Q = 1.037$ MHz and $\eta = 0.21$) for the N–H–N–H–N parts of the TNT molecules, including all the spins marked in the molecule diagram (figure 5). The dotted line in figure 5 shows predictions of the present description linking the shape of the proton magnetization curve to the geometry of the investigated molecule. Performing the detailed calculations for the H–N–H (figure 3) and N–H–N–H–N parts of the TNT molecule we use the geometrical parameters from [14]. We have used the N–H distance of 2.5 Å. The

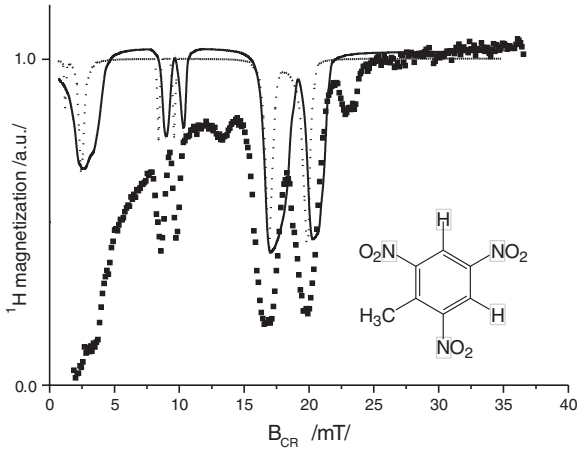

Figure 5. Experimental and calculated proton magnetization as a function of the cross-relaxation magnetic field B_{CR} for the N–H–N–H–N part of the TNT molecule (marked in the molecule diagram); squares—experimental data for the cross-relaxation time $t_{CR} = 8$ s. The theoretical prediction is shown as a dotted curve: $a_Q = 1.04$ MHz $\eta = 0.21$. The solid curve presents an overlapping of six curves corresponding to six pairs of quadrupole coupling parameters (given in the text) for TNT—solid curve.

angles between the dipole–dipole axes corresponding to the couplings of a given nitrogen spin to the two neighbouring protons lie between 117.5° and 125.5°. The orientation of the electric field gradient in the nitro groups is described in section 4.1.

The nitrogen NQR frequencies, quadrupole coupling constants and asymmetry parameters of military-grade TNT at room temperatures have been investigated and presented in [15]. According to this work, one can distinguish six positions of the nitrogen nuclei, characterized by the following pairs of parameters (a_Q [MHz], η): (1.056, 0.303), (1.087 MHz, 0.170), (1.064, 0.208), (1.045, 0.253), (1.068, 0.172) and (1.052, 0.179). In figure 5 we also present the theoretical proton magnetization development resulting from a superposition of these six contributions, concluding that the agreement with the experimental data is reasonable.

The experimental magnetization curves also exhibit small dips around 13 and 33 mT, visible in figures 3 and 5. In [1] they have been attributed to lattice defects or eventually to impurities. They cannot be reproduced on the background of our model, taking into account the TNT molecular geometry.

The proton spins of the methyl group, omitted in the above considerations, also require some attention. We shift this discussion to section 5.

4.4. Urotropine

The structure of urotropine molecules $C_6H_{12}N_4$ requires taking into account a large ensemble of spins to describe properly the polarization transfer mechanisms. The experimental data for urotropine are collected in the range of the cross-relaxation magnetic field 60–95 mT, corresponding to single-quantum proton transitions. For the purpose of extracting information about the static quadrupole interaction from the experimental data we have limited ourselves to the H–N–H part of the molecule. We have used in our analysis the crystallographic data for urotropine from [16, 17], setting the proton–nitrogen distance to 1.8 Å. In the context of the highly simplified treatment of the urotropine molecule we have set the electric field gradient tensor parallel to the external magnetic field. The quadrupole coupling parameters

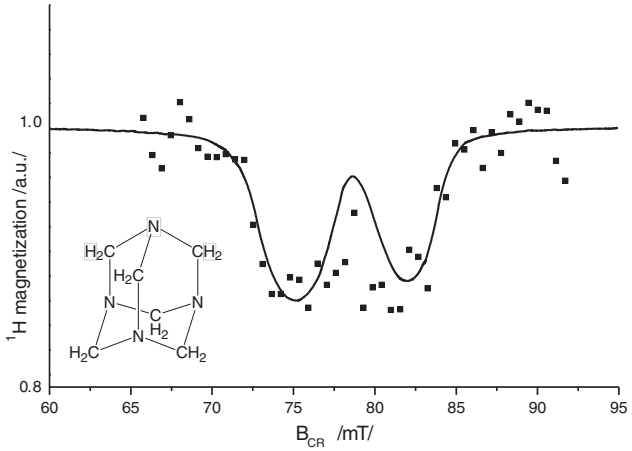

Figure 6. Proton magnetization for urotropine measured as a function of the cross-relaxation magnetic field B_{CR}, $t_{CR} = 0.5$ s (the group of spins H–N–H taken into account is marked in the molecule diagram). The theoretical prediction is shown as a solid curve: $a_Q = 4.43$ MHz, $\eta = 0.04$. In the magnetic field range chosen for the cross-relaxation experiment the proton magnetization transfer occurs through single-quantum proton transitions.

$a_Q = 4.43$ MHz and $\eta = 0.04$ correspond to the positions of the detected single-quantum dips and are in agreement with [14]: ($a_Q = 4.42$ MHz). The theoretical proton magnetization is compared with the experimental data in figure 6.

We wish to stress clearly that taking into account only the H–N–H spin system in our interpretation of the cross-relaxation experiments for urotropine is an oversimplification caused by computational limitations. However, the quadrupole coupling parameters obtained from the analysis of the H–N–H subsystems are valuable, reflecting the frequencies of the proton single-quantum transitions, which remain unchanged even if more spins contribute to the polarization transfer effects.

In the next section we discuss effects of non-equivalent spins involved in polarization transfers within one molecule (this subject has only been mentioned in the context of PNT and TNT) as well as a possible polarization transfer to neighbouring molecules. Some caution must be also exercised regarding field dependent relaxation processes in multi-spin systems, relevant for magnetization transfers.

5. Discussion

The presented approach provides a tool for a detailed understanding and analysis of polarization transfer processes in multi-spin systems containing spins $1/2$ as well as quadrupole spins. We have discussed the single- and double-quantum mechanisms of the polarization transfer as well as the effects of more spins participating in this process, using as an example a series of systems containing proton and nitrogen spins.

However, computational limitations of this approach should be emphasized. To analyse magnetization transfers between dipolar and quadrupole spins, one has to specify the group of spins involved in the magnetization transfer processes and relatively good isolated from the molecular environment. Since the number of spins which one can take into account is limited, it becomes a difficult task to extract an appropriate ensemble of spins. Choosing a group of spins relevant for an analysis of polarization transfers in molecular crystals, one

should try to find some compromises between the number of spins and the importance of information which one expects to get by enlarging the spin. In the illustrative calculations presented in section 4, we focus our attention on the physical mechanisms of magnetization transfer processes. To discuss the spin transitions leading to the formation of magnetization dips we treat the molecules as being isolated, i.e. we do not consider polarization transfers to atoms of neighbouring molecules. Actually, the 'single-molecule' approximation is well motivated for the considered systems and gives us a reasonable picture of the magnetization transfer. For PNT, the distance between the proton spins (which are involved in the intra-molecular polarization transfer) and nitrogen spins belonging to neighbouring molecules is 3.6–3.7 Å [10]. This value is larger than the inter-molecular proton–nitrogen distance. In the urea crystal lattice, molecules are linked together by hydrogen bonds, with the O–H distance between neighbouring ribbons of 2 Å [16]. According to [13] one can distinguish monoclinic and orthorhombic forms of TNT crystals. The relevant proton–nitrogen distances between neighbouring molecules are about 3.1 to 3.2 Å, while the inter-molecular distance is of 2.5 Å.

The methyl protons in the PNT and TNT molecules also require some comments. In general, an increase of the number of protons relative to nitrogens leads to a decrease of the observed magnetization dips. In the TNT molecule the distances between the protons of the methyl group and the closest nitrogen spins (2.7 Å) are comparable to the H–N distances for the 'ring' proton spins. For the PNT molecule the methyl proton–nitrogen distances are much longer. We have not included the methyl protons in our analysis. One can expect that they exhibit significantly faster relaxation than the other protons, such that they lose the polarization mainly due to their relaxation. Fast dynamics of methyl groups has been discussed intensively in the literature, for example [18–21]. Since the applied cross-relaxation times are long (8 and 15 s), the assumption that the proton polarization of the methyl group is lost due to spin–lattice relaxation processes is well motivated. However, we cannot provide the relevant relaxation times. The relatively good agreement between the theoretical predictions and the experimental data can also be treated as a confirmation of this assumption.

The PNT molecule also possesses two protons more distant from the nitrogen; they are neglected in our consideration. The magnetization of the second-group protons can be effectively taken over neither by the nitrogen spin belonging to the same molecule nor nitrogen spins of neighbouring molecules; the relevant proton–nitrogen distances are too large. However, the magnetization could also be lost due to relaxation caused by the dipole–dipole coupling of the second-group proton spins to the methyl protons. The mutual dipole–dipole couplings are influenced by the fast dynamics of the methyl protons.

Urotropine is an example of a rather complicated system. The considered group of spins (H–N–H) does not reflect the ratio between the number of proton and nitrogen spins in urotropine molecules. Taking into account a third proton spin for keeping the proper ratio between proton and nitrogen spins does not solve the problem of selecting an appropriate spin group for the analysis of the polarization transfer, since such a spin group cannot be treated as being well isolated in the molecule.

Some comments concerning relaxation processes relevant for the discussion of polarization transfer effects are also appropriate here. So far, relaxation processes are not included in our considerations. The proton polarization can be transferred to nitrogen if there is an efficient static proton–nitrogen dipole–dipole coupling. The requirement that the mutual dipole–dipole interaction is sensed by the participating spins as being time independent means that eventual motional modulations of the relevant dipole–dipole coupling must be significantly slower than the proton as well as nitrogen spin relaxation. However, the quadrupole spin can exhibit a complex, field dependent multiexponential relaxation, caused by fluctuations of the quadrupole coupling. This complicated issue is beyond the scope of the present paper. Field dependent

relaxation processes of high spins have been considered in detail in the context of an electron spin in [22]. The proton spins can in turn relax through dipole–dipole couplings to other proton spins in their environment, if the mutual dipole–dipole couplings are modulated fast enough by the lattice dynamics. It is important to realize that the fast fluctuations of proton–nitrogen dipole–dipole couplings can also provide a source of relaxation for both spins. However, if they are efficient for the relaxation processes due to their fast time modulations, they are not active in the polarization transfer processes.

The observed proton magnetization dips are modulated in a complicated manner by relaxation of the nitrogen as well as proton spins. The effects become visible especially if comparing results of the cross-relaxation experiments performed for different cross-relaxation times t_{CR}. An interplay between various relaxation channels can lead to interesting features of the magnetization curves. Performing the cross-relaxation experiment for urotropine we varied the cross-relaxation time t_{CR}, observing a significant effect on the dip shapes. To present in figure 6 the agreement between the theoretical positions of the CR dips (predicted for the given a_{Q} and η) and the experimental ones, we used intentionally the set of data where the observed dip depths fit to the theoretical ones obtained for the H–N–H subsystem, neglecting relaxation.

However, we think that cross-relaxation experiments performed for various t_{CR} from the point of view of protons as well as quadrupole spins together with field-dependent proton and quadrupole relaxation studies can provide a deep understanding of lattice dynamics and spin interactions, so it might be worthwhile to discuss the combined effects in a forthcoming paper.

6. Conclusions

This paper provides a theoretical tool for a detailed understanding and analysis of cross-relaxation experiments in multi-spin systems containing spins $1/2$ as well as quadrupole spins. The proposed approach links the efficiency of polarization transfer effects to molecular geometry. It can be adapted to an arbitrary molecular system in a straightforward manner. We discuss single- as well as double-quantum mechanisms of the proton polarization transfer for systems containing several proton and nitrogen spins. Illustrative calculations are presented for the series of spin systems H–N, H–N–H, N–H–N and H–N–H–N–H, involved in magnetization transfer processes in PNT, TNT, urea and urotropine molecules.

Acknowledgments

We would like to thank A Efremov from Kaliningrad State University, Russia for his support of our experimental work.

The study has been sponsored by Deutsche Forschungsgemeinschaft (grant FU 308/7-4).

References

[1] Nolte M, Privalov A, Altmann J, Anferov V and Fujara F 2002 *J. Phys. D: Appl. Phys.* **35** 939
[2] Rudakov T N, Belayakov A V and Mikhaltsevich V T 1997 *Meas. Sci. Technol.* **8** 448
[3] Garroway A N, Buess M L, Miler J B, Suits B H, Hibbs A D, Barrall G A, Matthews R and Burnett L J 2001 *IEEE Trans. Geosci. Remote Sensing* **39** 1108
[4] Fujara F, Stöckmann H-J, Ackermann H, Buttler W, Dörr K, Grupp H, Heitjans P, Kiese G and Körblein A J 1980 *Z. Phys.* B **37** 151
[5] Jäger E, Ittermann B, Sulzer G, Bürkmann K, Fischer B, Frank H-P, Stöckmann H-J and Ackermann H 1990 *Z. Phys.* B **80** 87
[6] Slichter P 1992 *Principles of Magnetic Resonance* 3rd edn (Berlin: Springer)

[7] Ernst R R, Bodenhausen G and Wokaun A 1987 *A Principles of Nuclear Magnetic Resonance in One and Two Dimensions* (Oxford: Oxford University Press)
[8] Kimmich R 1997 *NMR-Tomography, Diffusometry, Relaxometry* (Heidelberg: Springer)
[9] Varschalovisch D A, Moskalev A N and Khersonskii V K 1987 *Quantum Theory of Angular Momentum* (Singapore: World Scientific)
[10] Barve J V and Pant L M 1971 *Acta Crystallogr.* B **27** 1158
[11] Hiyama Y and Brown T L 1981 *J. Chem. Phys.* **75** 114
[12] Godfrey P, Brown R and Hunter A 1997 *J. Mol. Struct.* **413** 405
[13] Landolt-Börnstein 1988 *Numerical Data and Functional Relationships in Science and Technology* vol 3.3.20.a (Heidelberg: Springer) p 160, 244
[14] Miller G R and Garroway A N 2001 A review of the crystal structures of common explosives *Naval Research Laboratory* NRL/MR/6120-01-8585
[15] Blinc R 2001 *Workshop on NQR in Mine Detection (Joint Research Center Ispra, Italy, Oct. 2001)*
[16] Kampermann S P, Sabine T M, Craven B M and McMullan R K 1995 *Acta Crystallogr.* A **51** 489
[17] Gardon M, Schönleber A, Chapuis G, Hostettler M and Bonin M 2001 *Acta Crystallogr.* C **57** 936
[18] Dong S, Ida R and Wu G 2000 *J. Phys. Chem.* A **104** 11194
[19] Van der Putten D, Diezemann G, Fujara F, Hartmann K and Sillescu H 1992 *J. Chem. Phys.* **96** 1748
[20] Borst D R and Pratt D W 2000 *J. Chem. Phys.* **113** 3658
[21] Beckmann P A, Dybowski C, Gaffney J E, Mallory C W and Mallory F B 2001 *J. Phys. Chem.* A **105** 7350
[22] Kruk D, Nilsson T and Kowalewski J 2001 *Phys. Chem. Chem. Phys.* **3** 4907